Experimental Discharge Characterization and Scaling of IEC Plasma Devices

IEPC-2013-289

Presented at the 33rd International Electric Propulsion Conference, The George Washington University, Washington, D.C., USA
October 6–10, 2013

Constanze Syring* and Georg Herdrich†
University of Stuttgart, Stuttgart, 70567, Germany

Inertial electrostatic confinement (IEC) is considered to be a promising future technology for space applications especially for advanced space propulsion systems with high Isps. Since this technology was mainly investigated and developed for applications as neutron source until a few years ago, a great potential and need for investigations regarding discharge phenomena such as the propellant confinement and the jet extraction for thrust generation is still existent. Moreover, the mechanisms behind the different discharge phenomena are not deeply understood yet. However, there are theories giving an insight into the physics that still have to be confirmed by experiments. As part of an experimental applicability study of an IEC system three grid systems have been tested experimentally regarding discharge phenomena and discharge conditions. The grid fidelity have been varied regarding grid opening size, electrode surface and electrode gap. Results show the respective operational conditions for several discharge modes in different gases for each grid setup and are compared with each other. The influence of electrode size and design on discharge conditions and phenomena is displayed as well. Characteristic discharge behavior of propellants such as argon, nitrogen and helium could be observed.

*Research Associate, IRS - Institute of Space Systems, syring@irs.uni-stuttgart.de .
†Head of Electric Propulsion and Reentry Technology, IRS - Institute of Space Systems, herdrich@irs.uni-stuttgart.de.

I. Introduction

INertial electrostatic confinement devices have been investigated and developed for several applications such as neutron sources for research laboratories or medical applications,[1,2] neutron radiography or baggage screening.[3] In 2000 the research group of the University of Illinois patented an IEC plasma jet source.[4] The future application as space propulsion device in fusion and non-fusion mode was addressed afterwards systematically,[5,6] numerically[7] and experimentally[8] at different institutions. In 2012 the project HIIPER dealing with the characterization of a coupled Helicon source- IEC accelerator was introduced as advanced space propulsion system in non-fusion mode.[9–11]
Since 2011 a research campaign is ongoing at IRS investigating the applicability of IEC for space propulsion devices in a non-fusion mode as well. Three phases have been identified dealing with the deepened understanding of the confinement, the understanding how the jet extraction works and the design of a propulsion laboratory model separated from the test facility. For each of these phases plasma diagnostic methods are used in order to obtain plasma parameters which are also input parameter for numerical simulations. A numerical study has been engaged in 2012 with ESA[12] in order to simulate the jet extraction and thus underpin partially but also improve the physical theory. Currently three different grid setups are under investigation in the IRS laboratory with different dimensions and fidelity levels with respect to discharge phenomena and behavior. Additionally to argon, helium and nitrogen were used as propellants. The obtained data is presented in this paper.

II. Operational Modes

The operating principle of IEC was explained in depth in former publications,[13,14] which is why it is only introduced briefly. The IRS device consists of a spherical, concentric two-grid system. The outer grid, being the anode and the inner grid biased as cathode. Plasma is generated by glow discharge and ions are accelerated by the negative cathode potential into the inner grid center. They pass through the cathode and get accelerated into the center again. If ion energies are sufficiently high occasionally fusion processes can occur. Electrons inside the cathode are generated by ions passing through the cathode and ionizing the background gas by collisions, ion-grid collisions or glow emission of the cathode grid.
There are two operational modes under investigation at IRS. The *star mode* and the *jet mode*. The *star mode* (Figure 1 (a)) was discovered by the Miley group[13] and occurs if the grid is highly symmetric, has large grid openings and certain operation conditions (background pressure, discharge voltage and current) are given. The discharge phenomena features so called *microchannels* which are emanating from each grid opening. The *jet mode* occurs if a complete symmetry of the grid is not given, but one grid opening is larger than the others and certain operation conditions are commissioned. Here the "spray" *jet mode* (Figure 1 (c)) and "tight" *jet mode* (Figure 1 (b)) are distinguished. The conditions under which theses modes occur are under investigation.

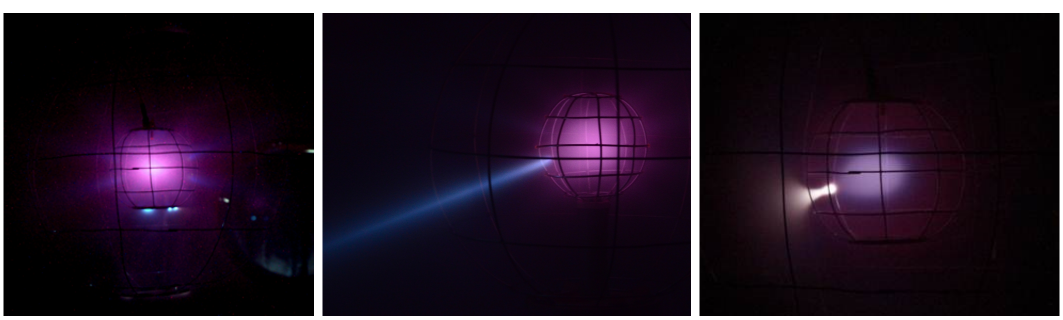

(a) *Star Mode* (b) "Tight" *Jet Mode* (c) "Spray" *Jet Mode*

Figure 1. Discharge Modes

III. Experimental Setup

The used vacuum facility is cylindrical, has a diameter of 1m and a length of 2.75m. The chamber is equipped with a fully automatic three-step pumping system providing an ultimate pressure of $10^{-5} mbar$. The operating pressure in the chamber is obtained by feeding gas into the chamber with a mass flow controller (Tylan). Chamber pressure (p_{ch}) is measured with a Pfeiffer Compact Full Range Gauge PKR 251.

The used power supply from FUG enables a voltage of max -3.5 kV and a current of 100 mA. Since the power unit only gives a rough display of voltage, a differential voltage probe (V) (Testec TT-SI 9110) is used to measure and scale down the voltage output transferring the data via a Datascan^{TM} system to a LabVIEW^{TM} acquisition program. Current (I) is measured by the voltage drop at a shunt implemented in the return line between anode and power supply (see Figure 3).

Three different grid setups were used for the discharge and scaling experiments (Table 1). Since scaling of spherical electrodes does not permit changing the electrode surface and the electrode gap separately, ratios are introduced in order to allow a better comparison. The first configuration (C1) is composed of an anode with 30 cm in diameter and a cathode of 10 cm and was hang up with nylon wires in the chamber. A second configuration C2a is composed of a 15 cm anode and a 5 cm cathode. The anode of C2a can also be combined with a 3.5 cm cathode which is C2b (Figure 2). In this case the grids are placed on PEEK holders. Grid setups C2a and b were manufactured in order to facilitate the manufacturing and therefore to increase the symmetry of the grids by reducing the size of the setup. Moreover, C2a was chosen to have the respective diameters in order to scale down the C1 setup by a factor of 2 and to keep the ratio of electrode gaps and electrode surfaces (anode/cathode). With the cathode of 3.5 cm the electrode gap in C2b can be varied, changing the ratio of electrode gaps and electrode surfaces. The number of longitude and latitude wires was maintained for all three configurations (5 latitude / 8 longitude). In that way the size of grid openings was reduced with C2a and C2b.

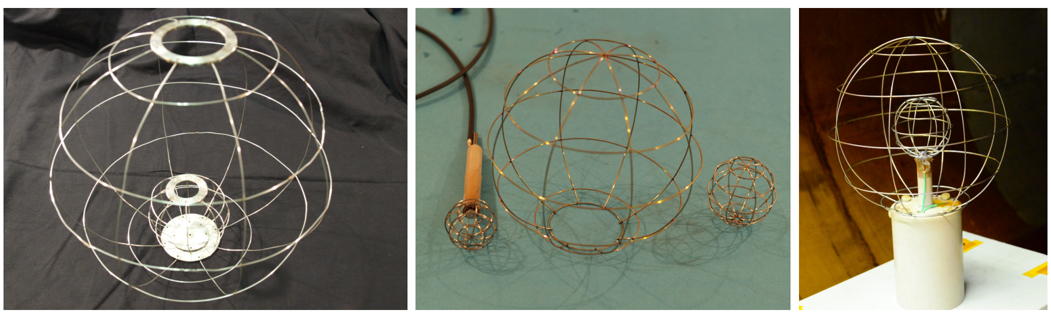

(a) C1 grids (b) C2b and C2a grids (c) C2a Setup

Figure 2. Grid Setups

	C1	C2a	C2b
Anode Diameter	30cm	15cm	15cm
Cathode Diameter	10cm	5cm	3.5cm
Electrode Gap	10cm	5cm	5.75cm
Gap Ratio	2		
		0.87	
Ratio Electrode Surfaces (A_A/A_C)	9	9	18.31

Table 1. Grid Configurations

For all setups the grid wires have a diameter of 1mm and are made of stainless steel, spot welded into spherical grids. The propellant used for the following tests are argon, helium and nitrogen.

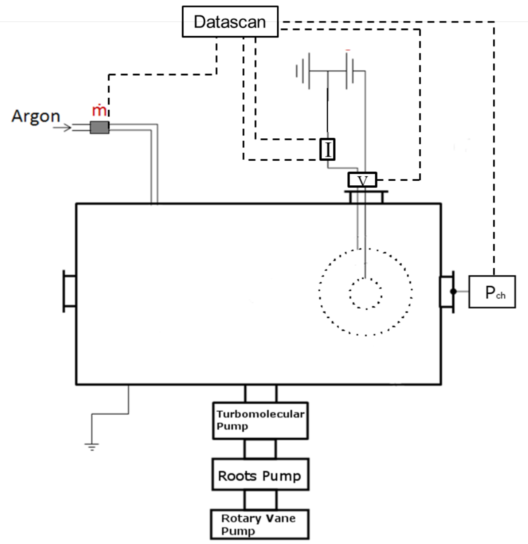

Figure 3. Experimental Setup

IV. Results

The following sections will present results of the discharge characterization for the three grid setups.

A. Grid Setup C1

Breakdown voltages and operational conditions for this configuration were already published in Ref.[15] But a better insulation, additional current and temperature measurements were performed by using an improved test setup. In that way this section will supplement the previous work.

Discharge Current Measurements

In this experimental setup discharge voltage and current are displayed by the power supply. Moreover voltage is measured by a voltage probe (Testec) at the voltage feed-through and discharge current by a shunt in the return line. Two pressure ranges were covered, $4 \cdot 10^{-3} - 8 \cdot 10^{-3}$ mbar and $4 \cdot 10^{-2} - 2 \cdot 10^{-1}$ mbar. The lower pressure range was tested for operational conditions with Argon shown in Figure 4. The curves named "PS" show data obtained from the power supply, which means these are the currents supplied by the source to the grid system in operation. The curves named "Shunt" show the data obtained in the return line. Although the grid system is isolated from the test facility, depending on the discharge a great deal of this supplied current does not flow back over the return line but through the ground of the vacuum chamber. Previous work regarding discharge phenomena in this setup[15] showed that the visible discharge phenomena spread out of the cathode with increasing discharge current. That could explain an increasing amount of current flowing via the chamber with increasing discharge power. This behavior was also observed for pressure levels between $4 \cdot 10^{-2}$ and $2 \cdot 10^{-1}$ mbar.

Discharge Phenomena

In previous experiments the pressure levels $4 \cdot 10^{-3} - 8 \cdot 10^{-3}$ mbar were not investigated regarding breakdown and discharge conditions and phenomena due to insulation issues. These have been improved by lining the chamber walls with capton foil. In Figure 4 the *V-I* characteristics for different pressures are given showing a voltage drop and current increase at the end of the curves for $5 \cdot 10^{-3}$ to $6.5 \cdot 10^{-3}$ mbar. This drop occurs if the discharge changes from a "tight" *jet mode* (Figure 1 (b)) in a "spray" *jet mode* (Figure 1 (c)), which indicates that the conductivity in the plasma rises with change in discharge mode. The "tight" *jet mode* was not observed with pressure levels $4 \cdot 10^{-2} - 2 \cdot 10^{-1}$ mbar only the "spray" *jet mode*.[15]

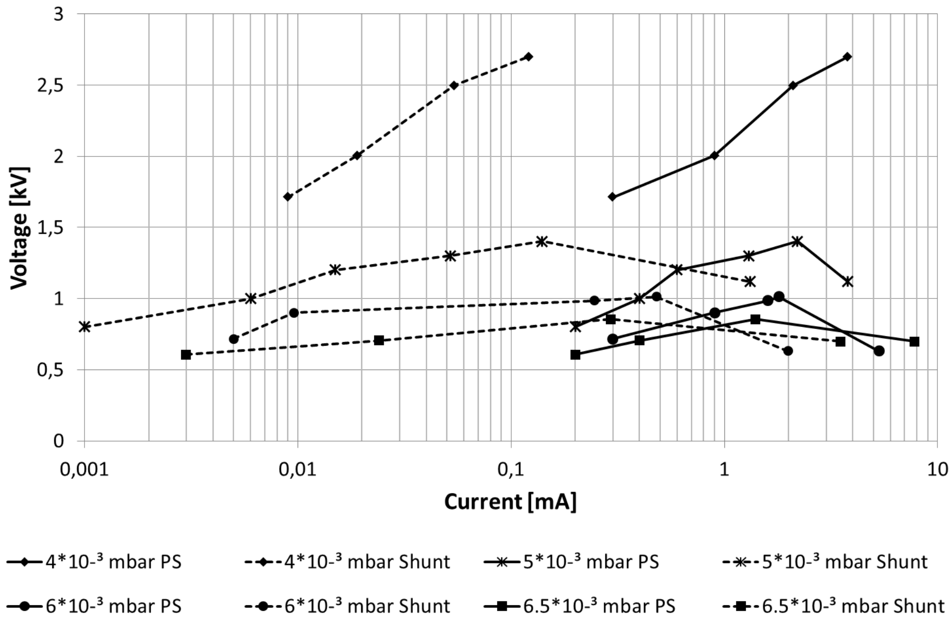

Figure 4. Operation conditions with current measurements via the power supply (PS) and a shunt in the return line for different pressure levels in Argon (C1)

B. Grid Setup C2a

This grid configuration was chosen in order to investigate firstly, whether the size of the grid openings does affect the discharge phenomena. And secondly to investigate the difference in discharge current and voltage depending on the electrode gap and size with respect to C1. Moreover this grid was tested with different fuels in order to assess dependencies on propellants regarding the discharge effects and conditions. Figure 5, 6 and 7 show the respective *V*-*I*-characteristics for argon, helium and nitrogen and photos of the distinctive discharge phenomena. The data of C1 that is used for comparison in this chapter is published in Ref[15] and won't be displayed in detail in this paper again. Note, that the pressure levels of the experiments with helium are different from those with nitrogen and argon which is attributed to the pumping capability of the used test facility. During operation with argon the PEEK holder got very hot due to heat dissipation from the grid resulting into melting processes on the holder surface. Nevertheless, all experiments could be finished with this setup.

Discharge Phenomena

Looking at the discharge phenomena and the different modes with respect to the reduced grid size opening of C2a, the comparison between C1 and C2a shows the following aspects:

- Some of the distinctive discharge phenomena that were observed with C1 in operation with argon[15] were also observed with C2a such as the visibility of faintly glowing plasma channels through all grid openings additionally to the jet mode when operating with higher discharge currents at $1 \cdot 10^{-1}$ mbar, see Figure 6 (b) bottom.
- But no jumping jets were observed with C2a and one grid opening was prefered during all operation conditions for the jet mode with argon, helium and nitrogen. Consequently a stable operation was achieved.
- Only one jet was observed during all operation conditions which indicates a better confinement for all propellants. For C1 multiple "spray" jets were switched on with increasing discharge power.
- No vanishing of the distinctive discharge effects changing into an overall glow within the cathode and in the inter electrode space occurs such as it was observed for C1[15] for currents up to 80 mA. However

this effect might occur at higher power levels that could not be operated with the used power supply at the time.

Figure 6 (b) shows the jet extractions headed in a different direction as in Figure 5 (b) and 7 (b). The test with argon was the first to be performed. Afterwards the setup was turned into the other direction in order to allow a better visibility for the experiments with nitrogen and helium.

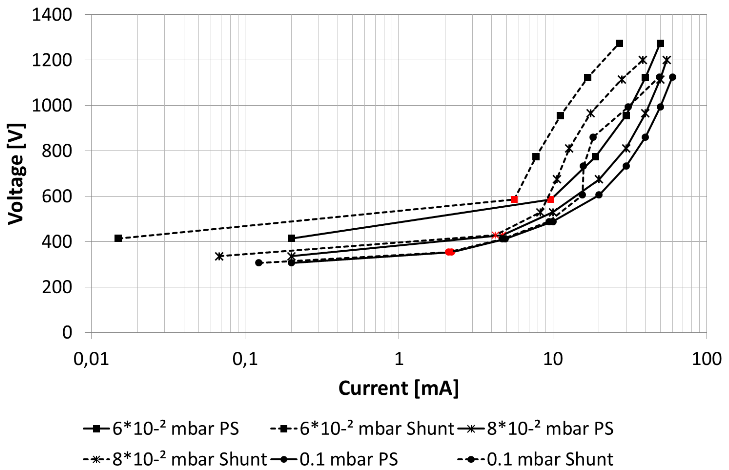

(a) Discharge conditions for several pressures, current measurement with power supply (PS) and shunt (transition between "tight" and "spray" *jet mode* in red)

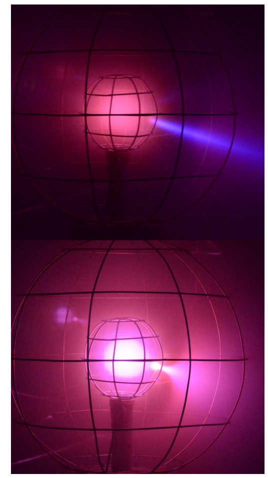

(b) C2a in "tight" *jet mode* (top) and "spray" *jet mode*(bottom)

Figure 5. Discharge conditions for nitrogen (grid setup C2a)

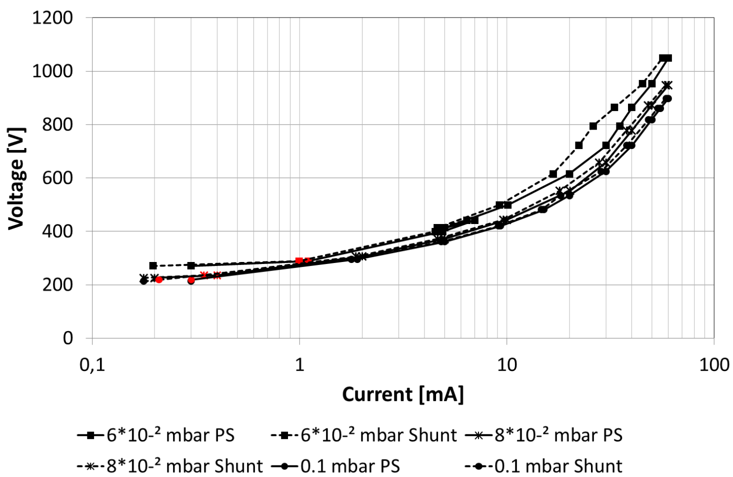

(a) Discharge conditions for several pressures, current measurement with power supply (PS) and shunt (transition between "tight" and "spray" *jet mode* in red)

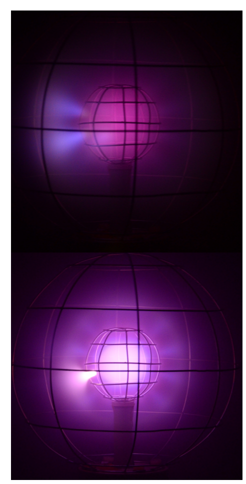

(b) C2a in diffuse "tight" *jet mode* (top) and "spray" *jet mode*(bottom)

Figure 6. Discharge conditions for argon (grid setup C2a)

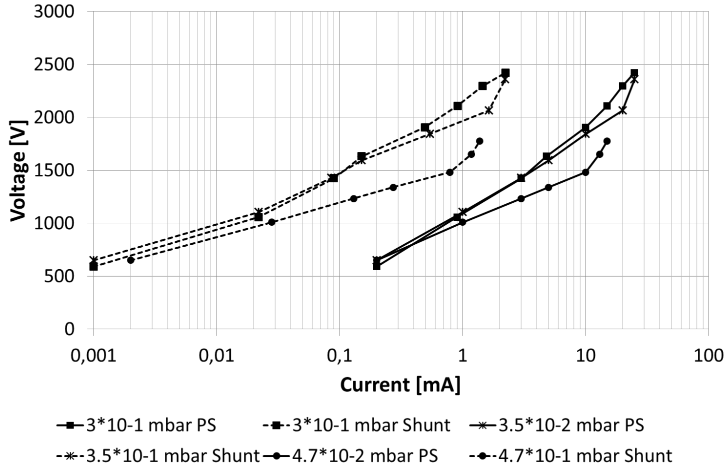

(a) Discharge conditions for several pressures, current measurement with power supply (PS) and shunt

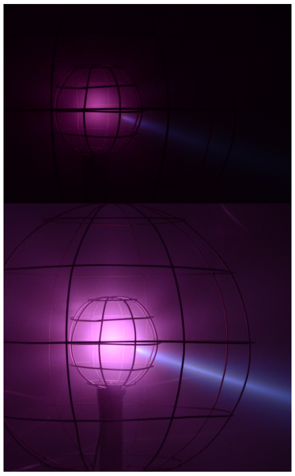

(b) C2a in "tight" *jet mode* (top and bottom)

Figure 7. Discharge conditions for helium (grid setup C2a)

Discharge Conditions

The impact of reduced electrode surfaces and electrode gap maintaining the same ratios (see Table 1) comparing C1 and C2a for argon is demonstrated in Figure 8 Here, only PS current measurements are shown. The results show:

- Higher voltages are needed to draw the same currents between the electrodes in C2a compared to C1, which is presumably caused by smaller electrode surfaces in C2a.

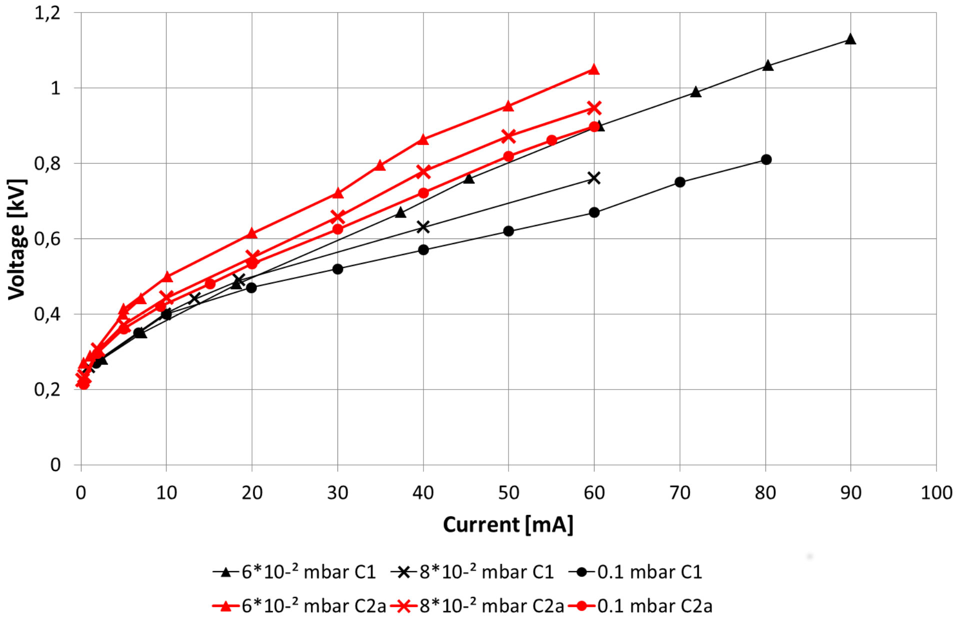

Figure 8. Discharge conditions of C1 and C2a for different argon pressure levels

Propellant

Considering the influence of different propellants for C2a, the obtained data shows:

- The transition between "tight" *jet mode* and "spray" *jet mode* was only observed with argon and nitrogen within the limit of the supplied power by the power source. For helium this transition might occur at higher power levels, but was not observed in these experiments. That might be influenced by the different ionization energies of the propellants, argon having 15.76 eV, nitrogen 14.53 eV and helium 24.59 eV.[16] In Figure 5 (a) and 6 (a) the red marked data points show the transition point between both modes.

- The transition point occurs at lower power for argon compared to nitrogen for all investigated pressure levels.

- Argon shows a much lower difference between "PS" current and "Shunt" current than nitrogen. The reason for that is not yet clarified and has to be investigated further.

- The "tight" *jet mode* is more diffuse for argon than for nitrogen and especially than for helium.

- Only helium shows a very distinct "tight" jet that reaches far out of the grid setup at the chamber wall (see Figure 9). The divergence only increases slightly with increasing background pressure.

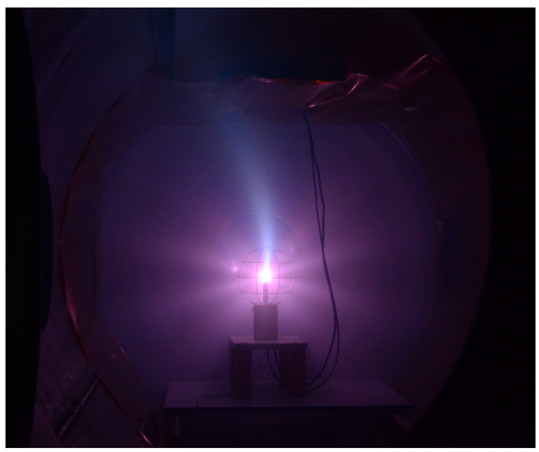

Figure 9. Helium jet attaching to the chamber wall

C. Grid Setup C2b

Grid setup C2b is used in order to compare it with C2a. The electrode gap is increased in C2b by keeping the anodes diameter at 15cm and sizing the cathode 3.5cm. Consequently this reduces also the grid opening size, since the number of latitude and longitude wires is kept the same as for C1 and C2a. Figure 10, 11 and 12 show the respective data for nitrogen, argon and helium. The same pressure levels were used as for the experiments with C2a. In order to avoid melting of the PEEK holder a ceramic washer was placed between cathode grid and holder, which worked quite well as heat isolator.

Discharge Phenomena

Comparing the discharge effects of C2a and C2b the reduction of the cathode surface and increased electrode gap show the following results:

- Faintly glowing plasma channels in all grid openings additionally to the "spray" jet were observed for C2b at higher currents and $1 \cdot 10^{-1}$ mbar as well as for C1 and C2a.

- No major differences in discharge phenomena were observed compared to C2a.

- No jumping jets, which are caused by an unstable operation, were observed with C2b and one grid opening was preferred during all operation conditions for the jet mode with the used propellants as it was also the case for C2a. The operation was stable.

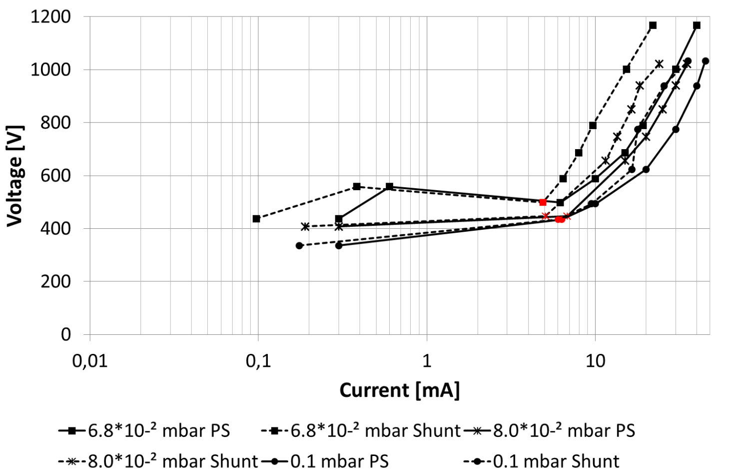

(a) Discharge conditions for several pressures, current measurement with power supply (PS) and shunt (transition between "tight" and "spray" *jet mode* in red)

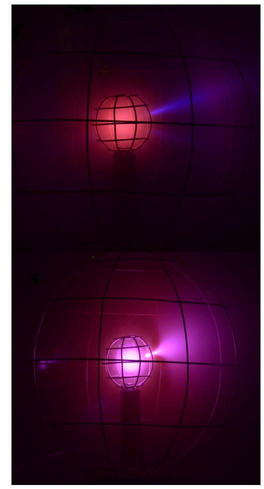

(b) C2b in "tight" *jet mode* (top) and "spray" *jet mode*(bottom)

Figure 10. Discharge conditions for nitrogen (grid setup C2b)

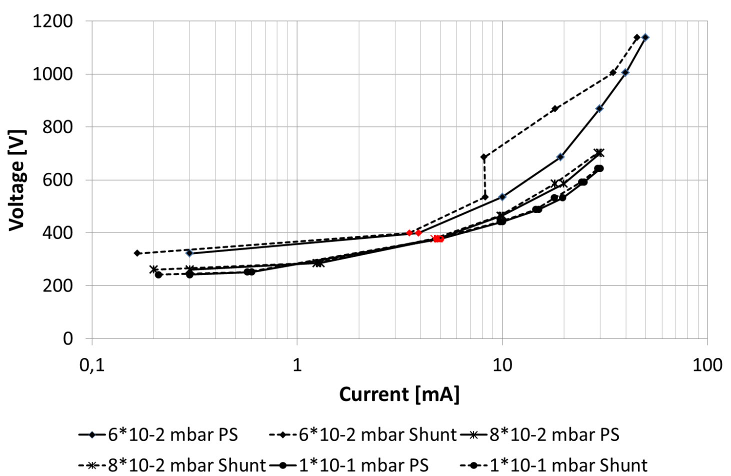

(a) Discharge conditions for several pressures, current measurement with power supply (PS) and shunt (transition between "tight" and "spray" *jet mode* in red)

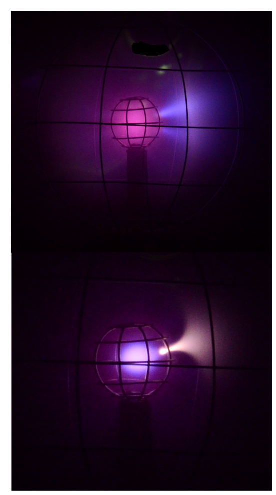

(b) C2b in "tight" *jet mode* (top) and "spray" *jet mode*(bottom)

Figure 11. Discharge conditions for argon (grid setup C2b)

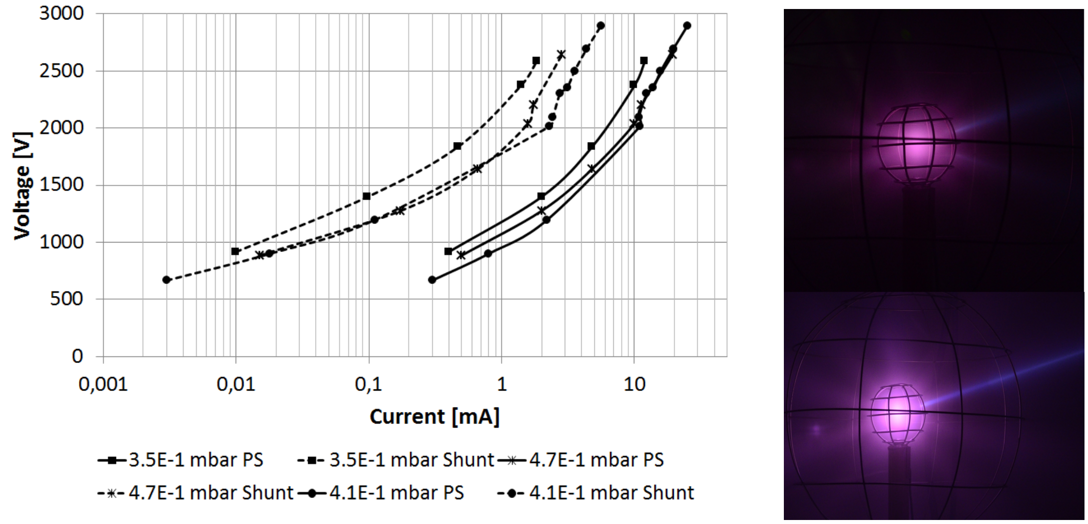

(a) Discharge conditions for several pressures, current measurement with power supply (PS) and shunt

(b) C2b in "tight" *jet mode* (top and bottom)

Figure 12. Discharge conditions for helium (grid setup C2b)

Discharge conditions

Discharge voltage and current of C2a and C2b are displayed in Figure 13. Here, only the power supply current and voltage measurement are shown (respective shunt data is shown in Figure 6, 7, 11 and 12).The discharge conditions of C2b and C2a compared to each other show the following aspect:

- From the data for argon and helium it is evident that the grid setup C2b, with a slightly larger electrode gap but a much larger ratio of electrode surfaces, needs a higher voltage to draw the same current between the electrodes.

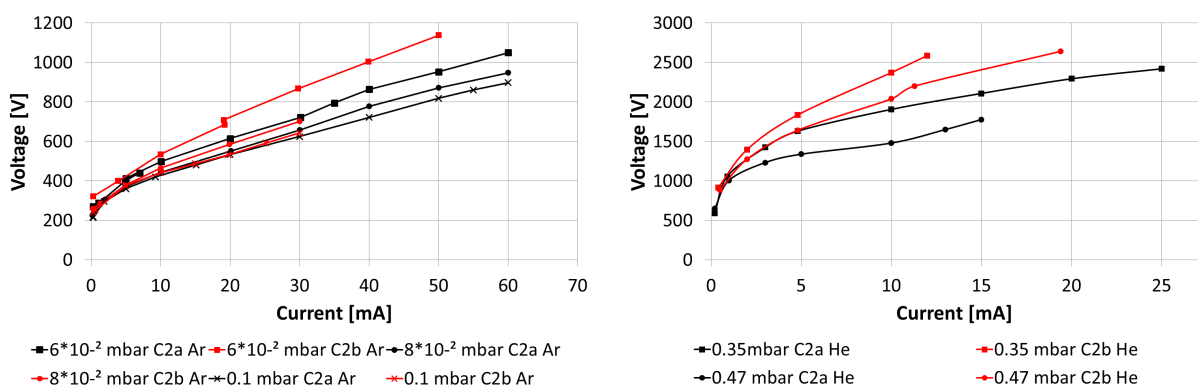

(a) Argon

(b) Helium

Figure 13. Comparision of discharge conditions (PS) for C2a and C2b

Propellant

Influences caused by the used propellant were the same as for C2a. Having only a "tight" *jet mode* for helium and a transition from "tight" *jet mode* to "spray" *jet mode* for argon and nitrogen occurred also for this grid setup.

V. Summary and Outlook

For all experiments the difference between power supply and shunt current measurement was observed rising with increasing supplied power to the grid system. If the difference actually flows via the chamber will be investigated in future experiments with an adjusted measurement setup, e.g. with hall probes measuring at the grounding line of the chamber.

For grid setup C1 the "tight" *jet mode* was observed at low pressures between $4 \cdot 10^{-3}$ to $8 \cdot 10^{-3}$ mbar, followed by the transition into the "spray" *jet mode*. The "tight" *jet mode* was not observed for pressure levels between $4 \cdot 10^{-2}$ to $2 \cdot 10^{-1}$ mbar.

C2a showed a very stable discharge behavior and better confinement, justified by only one jet occurring during all operational conditions for all used propellants. Moreover the "tight" *jet mode* was also observed at pressure levels between $4 \cdot 10^{-2}$ to $2 \cdot 10^{-1}$ mbar for argon, nitrogen and helium. A transition into the "spray" *jet mode* was only observed for argon and nitrogen.

C2b equipped with a smaller cathode showed no difference in discharge phenomena to C2a. For all grid configuration discharge conditions were presented and compared. Grid configuration C2a and C2b have to be tested with background pressures $4 \cdot 10^{-3}$ to $8 \cdot 10^{-3}$ mbar.

The downscaling of C1 to C2a showed that the reduced electrode surfaces have an effect on the current drawn between those electrodes, even though that the ratio of electrode diameter and surfaces were kept constant. The same effect was observed for C2b compared with C2a in this case also increasing the electrode gap. However, at this point no quantitative information can be extracted since additionally the effect of manufacturing uncertainties has to be investigated. For example, with manufacturing a bundle of cathodes and test them under the same operation conditions.

Temperature measurements were performed at critical points of the grid system, e.g. at the C1 cathode grid which is hold by nylon fibers or the PEEK holder in C2a and C2b in order to avoid melting. In operation with helium heat dissipation to the holder was no issue since the flowing currents reached with the power source were not as high as with argon and nitrogen. Moreover, the operation of each grid setup during the first test was unstable at the beginning but got more and more stable with heating up of the electrodes caused by the flowing discharge current. Since the position of the thermocouples was different due to the melting of the PEEK holder further tests with thermocouples directly attached to the grid should be repeated in order to assess the effect of cold and hot electrodes.

Acknowledgments

The authors like to thank Dipl.-Ing. Matthias Lau and Till Gebhardt for their help during the experiment.

References

[1]Miley, G., Sved, J., "The IEC star-mode fusion neutron source for NAA- status ans next-step designs", *Journal of Applied Radiation and Isotopes*, Vol. 53, 2000, p. 779-783

[2]Cipiti, B.B; Kulcinski, G.L, "Embedded D-He Fusion Reactions and Medical Isotope Production in an Inertial Electrostatic Confinement Device", *Fusion Science and Technology*, Vol. 44, 2003, p.534 - 541

[3]J. Sved, N. Menduev, T. Firestone, "Applications for Gas-Plasma Target Neutron Generators", *International Topical Meeting on Nuclear Research Applications and Utilization of Accelerators*, 4-8 May 2009, Vienna, SM/EN-18

[4]Miley, G., Gu, Y., Bromley, B.P, Nadler, J., Sved, J.,"Plasma jet source using an inertial electrostatic confinement discharge plasma", Patent 6121569, 19.09.2000, USA.

[5]Hammond, W.E., Coventry, M., Hanson, J., Hrbud,I., Miley, G., Nadler, J., "IEC fusion: The future power and propulsion system for space", *AIP Conference Proceedings*, Vol. 504 (1), 2000, p.1572-1578

[6]Miley, G., Momota, H.; Wu, L.; Reilly, M.P; Burton, R.; Teofilo, V.L; Dell, D.; Dell, R.; Hargus, W.A, "Space probe application of IEC thrusters", *Fusion and Science Technology*, Vol. 56 (1), p. 533-539

[7]McGuire, T.J., "Improved lifetimes and synchronization behavior in Multi-grid Inertial Electrostatic Confinement Fusion Devices", Ph.D.- Dissertation, Aeronautics and Astronautics Dept., MIT, Cambridge, MA, 2007

[8]Dietrich, C., Eurice, L. J.; Sedwick, R. J., "Experimental Verification of enhanced confinement in a multi-grid IEC device", *Proceedings AIAA Joint Propulsion Conference*, 2008, Hartford, Connecticut, AIAA-2008-4760

[9]Krishnamurthy, A., Ulmen, B.A; Keutelian, P.; Chen, G.; Miley, G., "Helicon Injected Inertial Plasma Electrostatic Rocket (HIIPER): Experimental Proof of Principle", *Proceedings AIAA Joint Propulsion Conference*, 2012, Atlanta, Georgia, AIAA 2012-3957

[10]Ulmen, B.A., Keutelian, P.; Chen, G.; Krishnamurthy, A.; Reilly, M.P; Miley, G., "Investigation of Plasma Properties in a Helicon-Injected Inertial Plasma Electrostatic Rocket (HIIPER)", *Proceedings AIAA Joint Propulsion Conference*, 2012, Atlanta, Georgia, AIAA 2012-3867

[11]Krishnamurthy, A., Chen, G., Ulmen, B.A., Miley, G., "Numerical and Experimental Measurements in a Helicon-IEC Thruster", *Proceedings AIAA Joint Propulsion Conference*, 2013, San Jose, California, AIAA-2013-3830

[12]Herdrich, G., Pfeiffer, M., Syring, C., Petkow, D., "Kinetic modeling of the jet extraction mechanism in spherical IEC devices", *Proceedings International Electric Propulsion Conference*, 2013, Washington DC, USA, IEPC-2013-416

[13]Miley, G., Gu, Y., DeMora, J.M, Stubbers, R.A, Hochberg, T., Nadler, J., Anderl, R.A, "Discharge Characteristics of the spherical inertial confinement (IEC) device", *IEEE Transactions on Plasma Science*, Vol. 25 (4), 1997, p.733-739

[14]Syring, C., Herdrich, G., "Development activities of an inertial electrostatic confinement device for space applications", *Proceedings International Astronautical Congress*, 2012, Naples, Italy, IAC-12-C4.7-C3.5.8

[15]Syring, C., Herdrich, G., "Development activities of an inertial electrostatic confinement device for space applications", *Proceedings of the AIAA Joint Propulsion Conference*, San Jose, California, 2013, AIAA-2013-4025.

[16]NIST Atomic Sprctra Database: http://www.nist.gov/pml/data/asd.cfm